Chemistry SELECT

www.chemistryselect.org

A journal of ChemPubSoc Europe

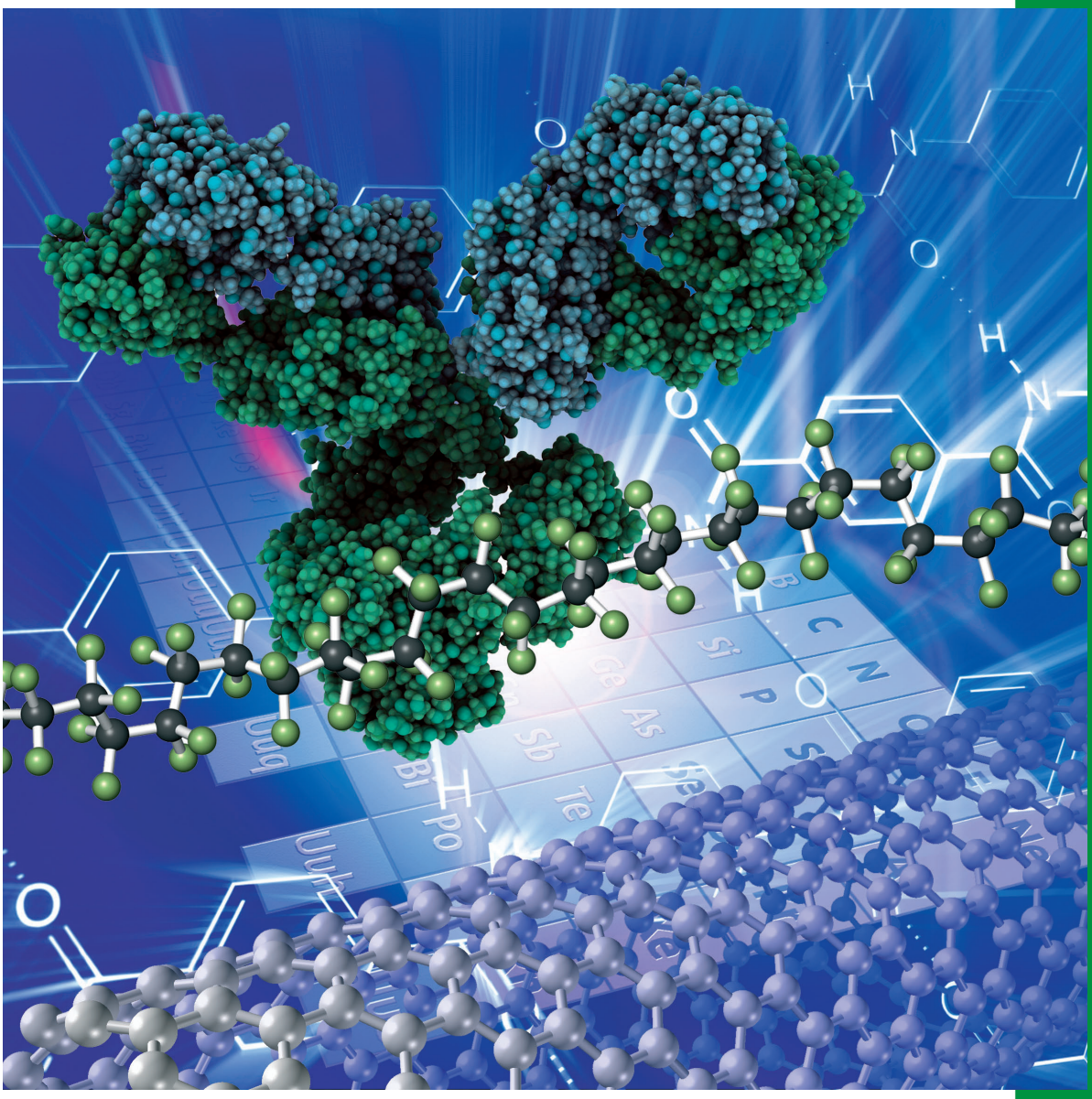

REPRINT

WILEY-VCH

ChemPubSoc Europe

DOI: 10.1002/slct.201801900

Chemistry SELECT Full Papers

Organic & Supramolecular Chemistry

Peptidomimicry with C_2-Symmetric Oligourea Derivatives of 1,2-Diaminocyclohexane and 1,2-Diphenyl-1,2-diaminoethane: Chirality and Chain Length-Dependent Conformation

Pengyun Yue[+],[a] Siqing Peng[+],[a] Sean Parkin,[b] Tonglei Li,[c] Faquan Yu,*[a] and Sihui Long*[a]

To study whether C_2 symmetric oligoureas form secondary structures such as sheets and helices/turns to serve as peptidomimetics, conformations of oligoureas composed of 1,2-diaminocyclohexane and 1,2-diphenyl-1,2-diaminoethane were investigated using X-ray diffraction, UV, CD and NMR spectroscopic methods. Alternating heterochiral diamines in these chains strongly favored helical conformations. The conformations of C_2-symmetric chains of homochiral diamines were more conditional, giving indications of conditional extended and helical structure.

Introduction

The mimicking of natural peptides, both structurally and functionally, with artificial oligomers is referred to as peptidomimicry.[1–6] The end products are called peptidomimetics.[7–9] Various strategies, such as cyclization of linear peptides,[10–12] replacing the natural amino acids with unnatural ones,[13–16] substitution of the amide functionality with other functional groups etc.,[17] have been applied to construct peptide mimetics. One particularly important category of peptidomimetics are foldamers[18,19] since they adopt/fold into secondary structures such as extended sheets or helices, analogous to natural peptides. Great success has been achieved in emulating both the higher structures and function of peptides with both unnatural peptides[20–30] and oligoureas.[31–40]

Although the approaches to address peptidomimicry abound, most of these artificial oligomers possess no symmetry and in general they have to reach a certain length to simulate natural peptides. Molecular C_2-symmetry could potentially simplify peptidomimetic chains and broadly conserve the conformational diversity observed in natural peptide chains. Clayden and coworkers have performed some studies based on cis-1,2-diaminocyclohexanes[41–43] and both cis- and trans-1,2-diaminocyclohexanes are incorporated into helix forming oligoureas to study its effects on the overall secondary structures of the parent molecules.[44] Yet in general, these oligoureas don't have a global C_2-symmetry. In this study, we investigated the suitability of C_2-symmetric oligoureas (both homochiral and heterochiral) to function as peptide conformational analogues. This account probes the dependence of global conformation on the chain length and the chirality of the constituent 1,2-diaminocyclohexane (**1**), and 1,2-diphenyl-1,2-diaminoethane (**2**), residues.

Relevant to this study, D-residue substitution in natural peptides induces turn conformation,[45–53] and local asymmetry in a chiral residue propagates global chiral conformation in biomimetic chains.[54–56] Likewise, the heterochiral sequences, $\mathbf{1}^{S}(\mathbf{1}^{R}\mathbf{1}^{S})_n$, and analogous chains including **2** (Fig. 1), favored helical/turn conformation. Whereas the homochiral chains incorporating monomers **1** and **2** had conditional conformation and gave CD signatures indicative of equilibria between extended and helical conformations that were sensitive to temperature and solvent. This work complements studies of conformations of α-chiral oligoureas (Figure 1).[31–44]

Results and Discussion

Oligourea Synthesis. Optically pure (purity ≧99%) enantiomers of **1** and **2** were purchased commercially. A mono-protected / mono-activated derivative of **1** was prepared as the vehicle for chain elongation. Optically pure $\mathbf{1}^{R}$ (or $\mathbf{1}^{S}$) was mono-protected with *tert*-butoxycarbonyl (*t*-Boc); the other amino group was activated as the *p*-nitrophenylcarbamate (PNP). Coupling of *t*-Boc-$\mathbf{1}^{R}$-PNP and *t*-Boc-$\mathbf{1}^{R}$ gave bis-*t*-Boc-$(\mathbf{1}^{R})_2$ and subsequently dimer $\mathbf{1}^{R}{}_2$ after deprotection. Starting with optically pure **1**, **2**, or $\mathbf{1}^{R}{}_2$, addition of two equivalents of *t*-Boc-

[a] *P. Yue,[+] S. Peng,[+] Dr. F. Yu, Dr. S. Long*
Key Laboratory for Green Chemical Process of Ministry of Education, Hubei Key Laboratory of Novel Reactor and Green Chemical Technology, School of Chemical Engineering and Pharmacy, Wuhan Institute of Technology, 206 1st Rd Optics Valley, East Lake New Technology Development District, Wuhan, Hubei 430205, China
Tel.: (027) 87194980
E-mail: fyuwucn@gmail.com
Sihuilong@wit.edu.cn
longsihui@yahoo.com

[b] *Dr. S. Parkin*
Department of Chemistry, University of Kentucky, Lexington, Kentucky 40506, USA

[c] *Dr. T. Li*
Department of Industrial and Physical Pharmacy, Purdue University, West Lafayette, Indiana 47907, U.S.A

[+] *Pengyun Yue and Siqing Peng contributed equally to this work.*

Supporting information for this article is available on the WWW under https://doi.org/10.1002/slct.201801900

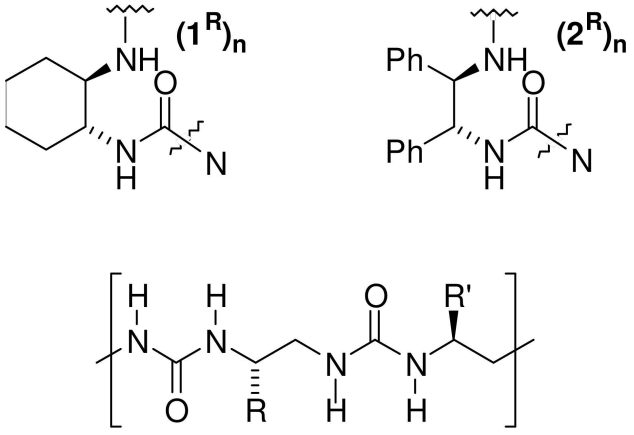

Figure 1. Chiral monomeric units incorporated in C_2 symmetric oligoureas. Related α-chiral oligoureas (bottom).

$\mathbf{1}^R$-PNP extended the chain by two units as shown in Figure 2. Subsequent deprotections and double elongations afforded

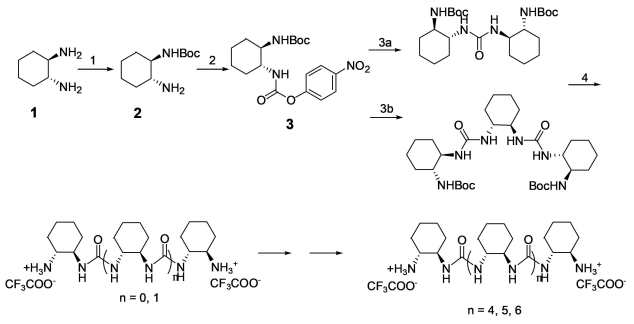

1. Boc_2O, CH_2Cl_2; 2. p-nitrochloroformate, pyridine, CH_2Cl_2; 3a.**2**, TEA, $CHCl_3$; 3b. **1**, TEA, $CHCl_3$; 4. CF_3COOH, CH_2Cl_2;

Figure 2. Double elongation solution-phase synthesis of homochiral oligoureas based on **1**.

the odd and even numbered chain lengths. Running these double elongations to completion simplified purification because separating chain length n from n+2 is much easier than separating chain length n from n+1. The alternate heterochiral oligoureas of **1** and **2** were synthesized with a similar strategy. Synthetic details are given in the experimental section. For convenience, $(\mathbf{1}^R)_7$ refers to the all-R homochiral heptamer, whereas $\mathbf{1}^R(\mathbf{1}^S\mathbf{1}^R)_3$ refers to the linear alternate-chirality chain: $\mathbf{1}^R\mathbf{1}^S\mathbf{1}^R\mathbf{1}^S\mathbf{1}^R\mathbf{1}^S\mathbf{1}^R$. When not indicated this shorthand refers to the free amine, when required, terminal functional groups are indicated in the abbreviation nomenclature.

Alternating heterochiral oligomers of **1** and **2** were more soluble than the homochiral oligomers as determined by UV-monitored dilution studies. Diamine $(\mathbf{1}^R)_7$* had aqueous solubility < 0.01 mg/mL, whereas the solubility of diamine heptamer, $\mathbf{1}^R(\mathbf{1}^S\mathbf{1}^R)_3$ was 1.7 mg/mL. One oligomer of similar constitution possessing more than 200x the solubility of the other was quite surprising. The tendency toward extended conformation in peptides often renders them intractable due to the intermolecular hydrogen bonding in β-sheet motifs.[57–60] X-ray studies showed that the oligoureas that preferred extended conformation had analogous hydrogen bonds between extended chains.

X-ray Diffraction. Chains longer than four residues of **1** or **2** did not produce diffraction-quality crystals, but the crystal structures of shorter n-mers were informative. Diammonium $\mathbf{1}^R\mathbf{2}^S\mathbf{1}^R$ (Figure 3, top left, CCDC 720589) and $\mathbf{1}^R\mathbf{1}^S\mathbf{1}^R$ (CCDC

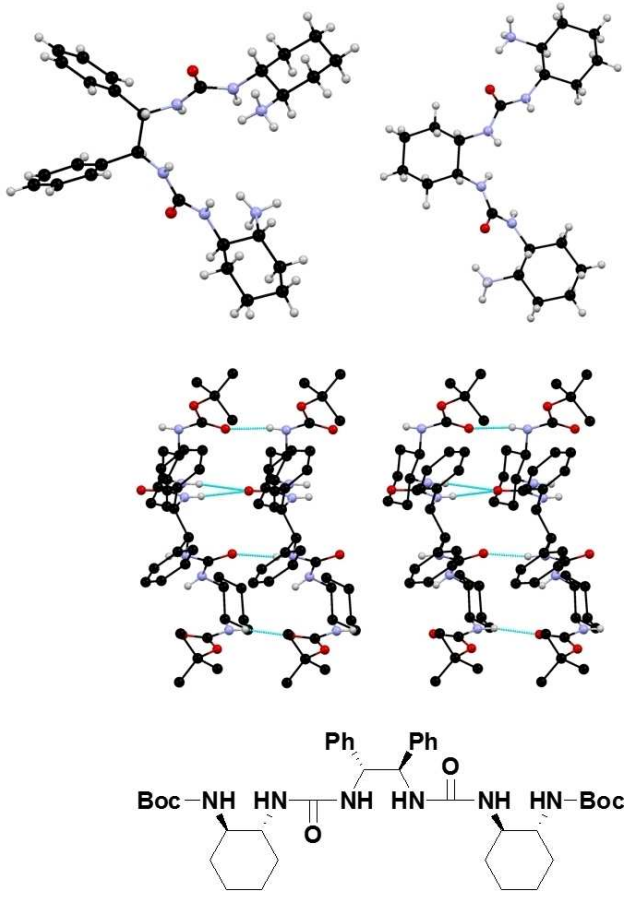

Figure 3. Top. Ball and stick conformation of trimeric diammonium trifluoroacetate salts (single crystal X-ray structures), $\mathbf{1}^R\mathbf{2}^S\mathbf{1}^R$•**2TFA** (top left, for clarity, TFA was omitted) is helical and $(\mathbf{1}^R)_3$ (top right) is extended. Middle: Stereo diagram of the X-ray crystal structure of $\mathbf{2}^R(\mathbf{1}^R\mathbf{t\text{-}Boc})_2$ showing hydrogen bonding between extended conformations. Bottom: Line structure of $\mathbf{2}^R(\mathbf{1}^R\mathbf{t\text{-}Boc})_2$.

1826468) crystallized in turn-like conformations. The two N-atom termini complete approximately one period about a putative helical axis. However *bis-t*-Boc$\mathbf{1}^S_3$•H_2O (CCDC 1826472), diammonium $\mathbf{1}^R_3$ (CCDC 1826469), and $\mathbf{2}^R(\mathbf{1}^R$t-Boc$)_2$ (Figure 3 top right and middle, respectively, CCDC 1826467) crystallized in extended conformations, stacked analogously to peptide β-sheets. The sequential urea carbonyls pointed in opposite directions in all the crystal structures.

The longest chains crystallized were the trifluoroacetate salt (TFA) of the pentameric $\mathbf{2}^R(\mathbf{1}^R\mathbf{1}^R)_2$ in the homochiral series

(Figure 4, top) and *bis*-cyclohexylamide-$\mathbf{2}^{S}(\mathbf{1}^{R})_2$ in the heterochiral series (Figure 4, bottom). Again the homochiral chain

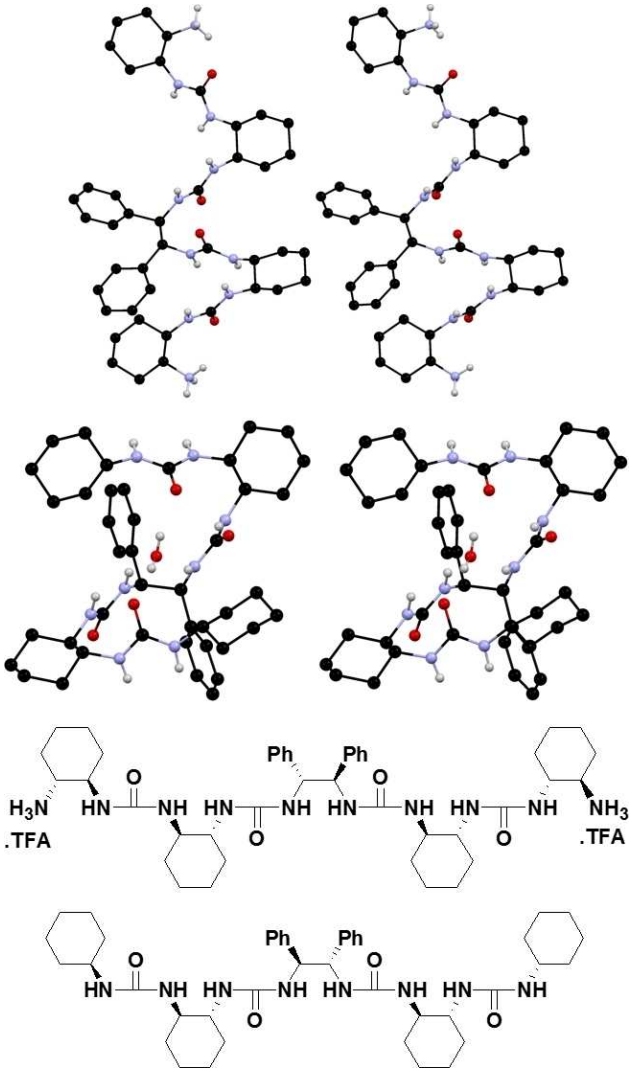

Figure 4. Stereo diagrams from X-ray diffraction. **Top**: extended conformation of $\mathbf{2}^{R}(\mathbf{1}^{R}\mathbf{1}^{R})_2$•2TFA (for clarity, TFA was omitted). **Bottom**: *bis*-cyclohexylamide of $\mathbf{2}^{S}(\mathbf{1}^{R})_2$•$H_2O$ (CCDC 1826478). The corresponding line structures are below.

crystallized in an extended motif and the heterochiral chain crystallized in a helical motif with a period of exactly 3 residues. As a likely consequence of the ionic bonds in the crystal lattice, $\mathbf{2}^{R}(\mathbf{1}^{R}\mathbf{1}^{R})_2$•2TFA (CCDC 1826470) did not neatly knit the extended chains together with hydrogen bonds between the urea functionalities as did the other extended conformations.

Definition of Extended and Helical Conformations: Figure 5 shows the limited conformational space occupied by the crystalline-state oligomers of **1** and **2** in a Ramachandran-like plot.[61] This graph is in terms of the dihedral angles ψ′ and ϕ′ defined below. As with the dihedral angles of amidic bonds in the Ramachandran plots of peptides, ω′, were ~180° and were not plotted.

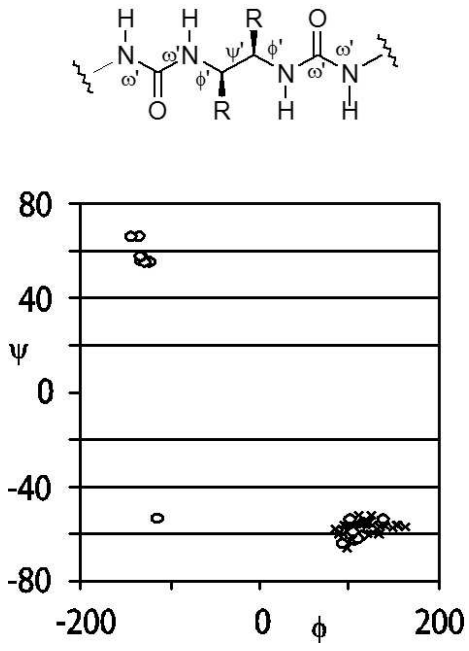

Figure 5. Top: Conformationally characteristic dihedral angles in C_2-symmetric oligoureas. Bottom: The dihedral angles are graphed from crystal states, homochiral-R, extended conformation = x and heterochiral helical = o. The lower left circle is residue **2** in *bis*-cyclohexylamide of $\mathbf{2}^{S}(\mathbf{1}^{R})_2$•$H_2O$.

Extended conformations of $\mathbf{1}^{R}{}_{n}$ occupy only the lower right region of the conformational space in Figure 5. The sign of ψ′ dihedral angles (~60°) in these chains depends on the chirality of the residues. The magnitude of ϕ′ is large in the extended chains, which disposes the atomic components 1 and 4 of these dihedral angles in a transoid relationship, shown in Figure 6, Top.

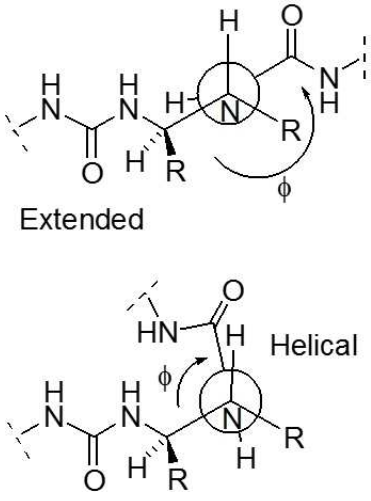

Figure 6. Top: ϕ angle mostly determines conformation. For extended chains of R chirality ϕ values are large (100-180°) and positive. For helical chains ϕ values alternate between negative and positive smaller values (100-110°).

Alternating heterochiral chains occupy the lower right and the upper left regions of the diagram because the ψ′ dihedral angles switch between ±60°, depending on the chirality of the diamine subunits and because smaller (~110°) ϕ′ angle values install gauche interactions in the chain, shown in Figure 6 (bottom). The ϕ′ angles are influenced less than the ψ′ angles by diamine residue chirality; changes in ϕ′ grossly determine whether the chain adopts a helical or extended conformation. A comparison between the torsion angles of the helical structures obtained in this study and reported helical structures [44] is shown in Table 1, indicating similarity between these structures.

Table 1. Main backbone torsion angles (deg) of the central unit in helical oligoureas in this study and a literature compound (from crystal structures)

oligourea	ϕ′	ψ′	ϕ′
$1^R1^S1^R$•2TFA	-132.21	+55.97	-124.33
$1^R2^S1^R$•2TFA	-134.88	+66.32	-143.54
bis-cylcohexylamide-1R2 S1R.H2O	-114.13	-53.27	-114.13
reference	-101.4	+54.4	+77.6

In heterochiral *bis*-cyclohexylamide of $\mathbf{2}^S(\mathbf{1}^R)_2$•$H_2O$ (CCDC 1826478), the diphenyldiamine moiety disposes the phenyl groups anti instead of gauche, which reverses the sign of ψ′ but not the sign of ϕ′, giving rise to the point in the lower left region of the graph. Homochiral chains $\mathbf{1}^R_n$ confine ψ′ to ~ −60°; extended conformations confine the sign of ϕ′ to large positive values (lower right). Putative helical conformations in $\mathbf{1}^R_n$ would have alternated the sign of ϕ′.

Solution State Conformation-CD. While circular dichroism spectroscopic studies cannot definitively indicate which global conformation is preferred, they showed that these oligomers adopt reversible secondary structures in solution, similar to native peptides. To unveil the synergy between residues necessary for secondary-like structures, we studied chain length dependence in CD spectra of $(\mathbf{1}^R)_n$, and $\mathbf{1}^R-(\mathbf{1}^S\mathbf{1}^R)_x$. The observed λ_{max} 195–205 nm was reminiscent of similar oligomers to which helical conformation was assigned.[62] Chromophoric aromatic residues complicate interpretation of the CD curves.[63,64] Thus, residue **2** was omitted to simplify the CD signature.

The curve in Figure 7 (bottom) is the absolute value of the molar ellipticity (top) for -$(\mathbf{1}^R)\mathbf{1}^S(\mathbf{1}^R)$- as a function of the number of residues in the chain. Only optically pure, odd numbers of residues are presented; the even chains are achiral. As units of alternate chirality are added to both termini, the sense of the global chirality alternates and the optical purity of the chain decreases: chain %ee = 1/n x 100%. This is consistent with the signal being dependent on the one extra disymmetric residue of alternating chirality, which mandates the handedness of the global conformation.

The CD spectra of this heterochiral family of oligoureas had the same signature (Figure 7 top). Thus there was little evidence for a global conformational switch as the chain elongated. However, if there had been no chain length-dependent conformation, molar ellipticity (ME) on the Y-axis of Figure 7 (bottom) should have decreased linearly with increasing chain length. However, the data indicated a cooperative,[57] residue-based, conformational effect that loses to decreasing chain optical purity after seven units.

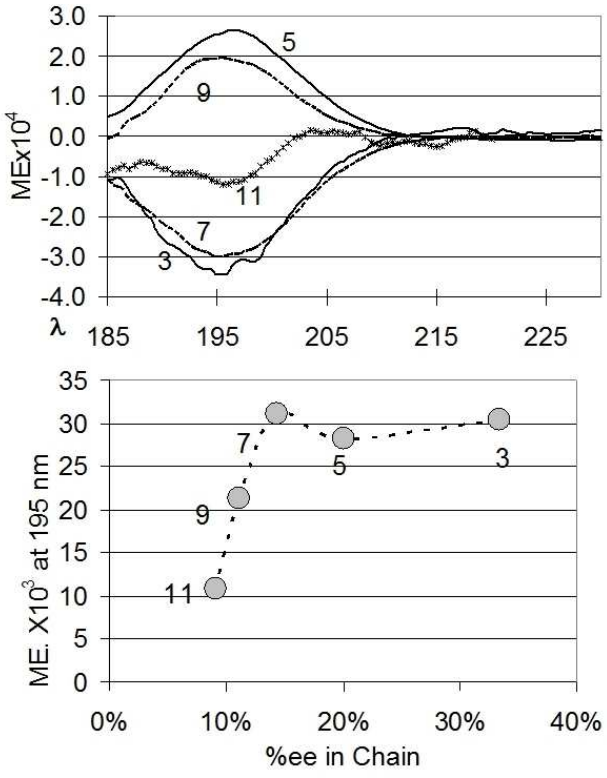

Figure 7. Top: CD molar ellipticities (ME) of $\mathbf{1}^R-(\mathbf{1}^S\mathbf{1}^R)_x$ at ca. 400 μM, 25° C in water. The corresponding chain lengths are labelled on the curve. **Bottom**: The *absolute value* of ME (above) at 195 nm vs. chain optical purity. Number labels on the points denote chain length.

The above CD evidence suggests that conformations in the heterochiral chains initiate in short sequences. The broad conclusions from this and the crystal structures point to dynamic conformations likely dominated by diastereomeric right- and left-handed helices with equilibrium constants approaching unity as the chains lengthen with concomitant losses in chain optical purity.

The CD spectra of the homochiral oligoureas in Figure 8 were more sensitive to changes in solvent and temperature than those of the homochiral series. These spectra change reversibly with temperature. A variable temperature CD study of $\mathbf{1}^R_8$ is included in the supporting information. Unlike the heterochiral sequences, which lose chain %ee with increasing chain length, the homochiral chains maintain chain %ee, so to understand the effect of the n^{th} residue it is necessary to average the effect of each residue. In Figure 8 the mean residue molar ellipticities (MRME) of a series of homochiral chains in MeOH are plotted.

Contrasting notably with the CD signatures of the heterochiral chains, the shapes of the CD curves change in the homochiral series as the chain lengthens from n = 3 to 5. This

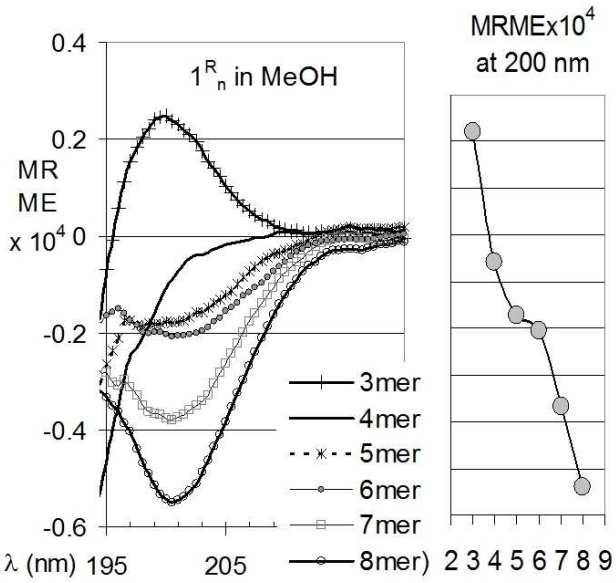

Figure 8. CD study of homochiral $(\mathbf{1}^{R})_x$. *Mean residue* molar ellipticities (MRME) were recorded as a function of chain length in MeOH.

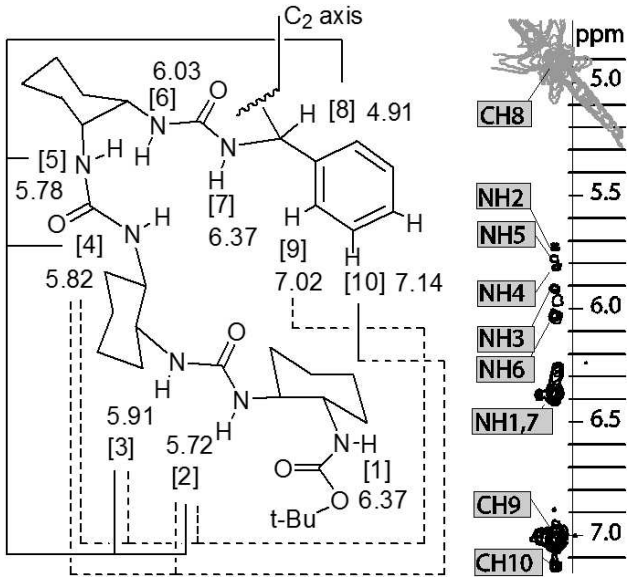

Figure 9. Long-range ROESY correlations between CH8 and numbered NH of $\mathbf{2}^{R}(\mathbf{1}^{S}\mathbf{1}^{R}\mathbf{1}^{S}t\text{-Boc})_2$ are evidence for helical structure.

shift in signature indicates a change in the global conformation, not just a shift in the equilibria between similar conformations. At approximately 3–4 residues, the spectral signature indicates a shift in conformational distribution—from X-ray structures, likely from linear to helical. Further lengthening of the chain causes increased changes in MRME, indicating more global structure per residue. Residue number 4 is the first one that overlaps on the helical axis in the crystal structure in Figure 3 (bottom), so it is not surprising that this chain length initiates a shift in global conformation.

A caveat with these experiments is the previously noted tendency of the homochiral chains to aggregate. However, due to the increased solubility, at 600–200 μM in MeOH instead of water, aggregation does not appear to be problematic. Dilution to the detection threshold did not change the CD signature.

Solution State Conformation-^{1}H NMR. CD spectra indicated that seven diamine units likely maximize the equilibrium constant between *putative* left- and right-handed helices in heterochiral $\mathbf{1}^{R}(\mathbf{1}^{S}\mathbf{1}^{R})_x$. The X-ray structures favored helical conformations of the heterochiral chains. It follows that in solution-state these molecules switch between diastereomeric L- and R-handed helices as they do in cyclic oligomers of α-amino acids.[50]

Between these two helices, analogous ^{1}H NMR signals are diastereotopic, but the magnetic dispersion of the cycloalkane chemical shifts of $\mathbf{1}^{S}(\mathbf{1}^{R}\mathbf{1}^{S}\mathbf{1}^{R}t\text{-Boc})_2$ was insufficient to use individual 2D NMR signals to determine conformation. However, diphenyl residue, **2**, at the axis of rotational symmetry in $\mathbf{2}^{R}(\mathbf{1}^{S}\mathbf{1}^{R}\mathbf{1}^{S}t\text{-Boc})_2$ provided unique signals and increased signal dispersion with magnetic anisotropy (600 MHz, DMSO-[d6] with ROESY-450 ms mix and TOCSY-45 ms mix). ROESY and TOCSY (supporting information) cross peaks allowed the spectral assignment shown in Figure 9. The primary structural, non-symmetry related NH chemical shifts are numbered starting at the chain terminus. The α-CH, and the aromatic *ortho* and *meta* H atoms of the diphenyl residues are designated H8-10 respectively.

NH1 and NH7 were almost isochronous under optimal conditions, so they contributed little to the analysis. The NH groups of specific 1,2-diamine residues had strong TOCSY cross peaks, but had weak ROESY cross peaks. On the other hand, the NH groups of specific urea functionalities had strong ROESY cross peaks but weak TOCSY cross peaks. This 2D spectral signature indicated a preference for *cis*-urea conformations that anti-align adjacent carbonyl groups. This interpretation is corroborated by atomic positions in all the crystal structures discussed above.

Evidence for helical structure in $\mathbf{2}^{R}(\mathbf{1}^{S}\mathbf{1}^{R}\mathbf{1}^{S}t\text{-Boc})_2$ comes from the presence of ROESY cross peaks between signals of NH2-NH5 and signals of CH8. These are corroborated weakly by analogous correlations with CH9. In helical structures (Figure 10) these H atoms are proximal, but in extended structures these H atoms are distal, beyond the ~5 Å nOe cutoff.[65]

Figure 10 depicts L- and R-handed helices; these structures are calculated energetic minima of conformational searching with nOe distance constraints in the force field AMBER*[66] which slightly favored the L-handed helix. The L- and the R-helices complete ~3 cycles over seven residues, which is the periodicity observed in the X-ray structure in Figure 3 (bottom). Calculations and the X-ray structure of $\mathbf{1}^{R}\mathbf{2}^{S}\mathbf{1}^{R}$**•2TFA** disposed the 1,2-diphenyl groups in **2** in a gauche conformation whereas the *bis*-cyclohexylamide of $\mathbf{2}^{S}(\mathbf{1}^{R})_2$•$H_2O$ disposed the 1,2-diphenyl groups in an *anti* conformation. Solution-state structures that dispose phenyl substituents *anti* would correlate phenyl H9 to H4 within 3.3 Å, and phenyl H10 to H4 within 2.7 Å. These cross peaks are quite strong (viz. X-ray structure

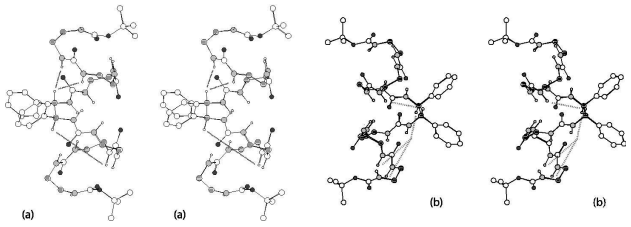

Figure 10. (a) Stereographic, calculated AMBER* left-handed, helical backbone of $\mathbf{2}^{R}(\mathbf{1}^{S}\mathbf{1}^{R}\mathbf{1}^{S}t\text{-Boc})_2$, showing the ROESY-detected proximities CH8-NH2 and CH8-NH3 (top). Distances CH8-NH4 and CH8-NH5 are out of nOe range (bottom). Some H atoms and the cyclohexane moieties were excluded for clarity; hatch = αC, and H; grey = N; and black = O. (b) Shows the corresponding right-handed helix in which key distal H/H correlations in (a) become proximal and *vice versa.*

and supplemental ROESY). Even though residue **2** obviously serves as a break point in the global conformation of $\mathbf{2}^{R}(\mathbf{1}^{S}\mathbf{1}^{R}\mathbf{1}^{S}t\text{-Boc})_2$, mixed R and L helices on either side of residue **2** are likely minorities in the conformational distribution due to conformational cooperativity across residue **2**. Taken together, a reasonable interpretation of the NMR data includes the conformations depicted in Figure 11 with L′ and R′ being minority conformations.

The dashed lines in Figure 10 indicate the short CH8-NH distances at the tops of structures **a** and **b**. The dashed lines at

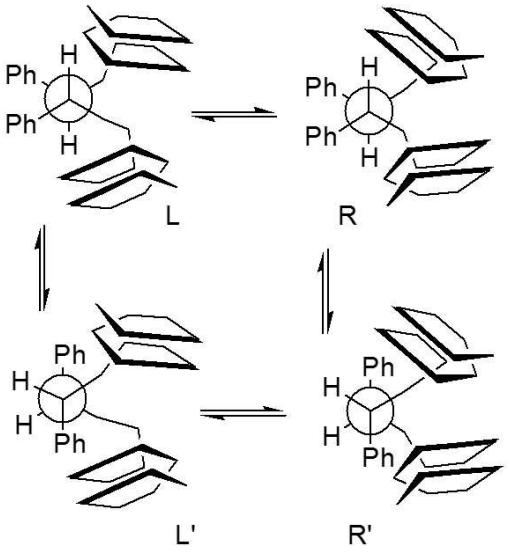

Figure 11. Schematic conformational distribution of the solution state of $\mathbf{2}^{R}$ $(\mathbf{1}^{S}\mathbf{1}^{R}\mathbf{1}^{S}t\text{-Boc})_2$.

the bottoms of both structures indicate the longer CH8-NH distances. Dynamic equilibrium between L- and R-helices explains the medium-intensity cross peaks between CH8 and the four NH signals. The L-helix has short CH8-NH2 and CH8-NH3 distances; in the R-helix these distances are long. Conversely, the R-helix has short CH8-NH4 and CH8-NH5 distances; in the L-helix these distances are long. These cross peak signals indicative of helicity would be more intense if a one-handed helix were present instead of splitting diastereotopic magnetization between two conformations. The highest-intensity cross peak (int = 1.2) in this set of four is the correlation between CH8 and NH3—a strong indicator of a 14-membered hydrogen-bonded ring in the L-helix. The second most intense cross peak (int = 0.9) in this set is the correlation between CH8 and NH4—indicating another 14-membered hydrogen-bonded ring in the R-helix. The corresponding four distances in the calculated low-energy extended coil are between 6.5 and 11 Å, which are well beyond the typical 5 Å nOe cutoff.[65]

In these studies, the conformations of Boc-terminated and free-amine chains in the crystalline state depended on whether the chain was homo or heterochiral. The crystalline state conformers did not depend on the chemistries of chain termination (capping). Thus, the conformational equilibria in the CD studies of the free amines and the NMR study of $\mathbf{2}^{R}$ $(\mathbf{1}^{S}\mathbf{1}^{R}\mathbf{1}^{S}t\text{-Boc})_2$ should differ in magnitude but not in kind. The effect of capping was not studied further.

Conclusion

This study shows that C_2-symmetric oligoureas encompass some of the conditional conformational behavior of natural peptides in terms of helical and extended conformation and in terms of a general conformational response to heterochiral substitution. Since helical structures and loops generally exclude reflection symmetry, C_2-symmetric oligomers like those reported herein are beguilingly simple peptide mimics. This raises questions about whether C_2–symmetric constructs could fold into protein-like, native states[67] and questions about how much molecular diversity such hypothetical constructs might afford.

Supporting Information Summary

Crystal structures of seven oligoureas in the form of crystallographic information file (CIF) were deposited in the Cambridge Crystallographic Data Centre (CCDC) with accession codes 1826467–1826472, 1826478 and 720589. This material is available free of charge *via* the Internet at https://www.ccdc.cam.ac.uk/.

Acknowledgment

SL is grateful to National Science Foundation of Hubei Province for financial support (2014CFB787), and thanks Dr. Arthur Cammers for helpful discussions. Crystallography at UK is supported by the NSF MRI program (CHE-0319176 and CHE-1625732).

Conflict of Interest

The authors declare no conflict of interest.

Keywords: Conformation · C_2 symmetric · oligourea · peptidomimetic · secondary structure

[1] Y. Ikeda, L. W. Schultz, J. Clardy, S. L. Schreiber, *J. Am. Chem. Soc.* **1994**, *116*, 4143–4144.
[2] Y. Odagaki, J. Clardy, *J. Am. Chem. Soc.* **1997**, *119*, 10253–10254.
[3] J. Xiao, B. Weisblum, P. Wipf, *J. Am. Chem. Soc.*, **2005**, *127*, 5742–5743.
[4] C. E. Oyiliagu, M. Novalen, L. P. Kotra, *Mini-Rev. Org. Chem.* **2006**, *3*, 99–115.
[5] D. W. Carney, K. R. Schmitz, A. C. Scruse, R. T. Sauer, J. K. Sello, *ChemBioChem.* **2015**, *16*, 1875–1879.
[6] K. S. Lam, M. Lebl, V. Krchnak, *Chem. Rev.* **1997**, *97*, 411–448.
[7] M. Goodman, R. Rone, N. Manesis, M. Hassan, N. Mammi, *Biopolymers.* **1987**, *26 Suppl*, S25-32.
[8] B. De, J. J. Plattner, E. N. Bush, H. S. Jae, G. Diaz, E. S. Johnson, T. J. Perun, *J. Med. Chem.* **1989**, *32*, 2036–2038.
[9] D. S. Kemp, *Trends Biotechnol.* **1990**, *8*, 249-255.
[10] J. N. Lambert, J. P. Mitchell, K. D. Roberts, *J. Chem. Soc.*, Perkin Trans. 1, **2001**, 471–484.
[11] C. J. White, A. K. Yudin, *Nat. Chem.* **2011**, *3*, 509–524.
[12] E. Marsault, M. L. Peterson, *J. Med. Chem.* **2011**, *54*, 1961–2004.
[13] A. Giannis, F. Rübsam, *Advances in Drug Research*, ed. T. Bernard and A. M. Urs, Academic Press, **1997**, vol. 29, p. 1 – 78.
[14] A. Grauer, B. König, *Eur. J. Org. Chem.* **2009**, 5099–5111.
[15] J.-M. Ahn, N. A. Boyle, M. T. MacDonald, K. D. Janda, *Mini-Rev. Med. Chem.* **2002**, *2*, 463–473.
[16] X. Li, Y. D. Wu, D. Yang, *Acc. Chem. Res.* **2008**, *41*, 1428–1438.
[17] I. Avan, C. D. Hall, A. R. Katritzky, *Chem. Soc. Rev.* **2014**, *43*, 3575–3594.
[18] S. H. Gellman, *Acc. Chem. Res.* **1998**, *31*, 173–180.
[19] D. J. Hill, M. J. Mio, R. B. Prince, T. S. Hughes, J. S. Moore, *Chem. Rev.* **2001**, *101*, 3893–4011.
[20] J. W. Checco, S. H. Gellman, *ChemBioChem* **2017**, *18*, 291–299.
[21] M. V. Hager, L. M. Johnson, D. Wootten, P. M. Sexton, S. H. Gellman, *J. Am. Chem. Soc.* **2016**, *138*, 14970–14979.
[22] R. W. Cheloha, T. Watanabe, T. Dean, S. H. Gellman, T. J. Gardella, *ACS Chem. Biol.* **2016**, *11*, 2752–2762.
[23] D. F. Kreitler, D. E. Mortenson, K. T. Forest, S. H. Gellman, *J. Am. Chem. Soc.* **2016**, *138*, 6498–6505.
[24] B. F. Fisher, L. Guo, B. S. Dolinar, I. A. Guzei, S. H. Gellman, *J. Am. Chem. Soc.* **2015**, *137*, 6484–6487.
[25] K. J. Peterson-Kaufman, H. S. Haase, M. D. Boersma, E. F. Lee, W. D. Fairlie, S. H. Gellman, *ACS Chem. Biol.* **2015**, *10*, 1667–1675.
[26] V. M. Kung, G. Cornilescu, S. H. Gellman, *Angew. Chem. Int. Ed.* **2015**, *54*, 14336–14339, *Angew. Chem. 127*, 14544–14547.
[27] Y. Demizu, M. Oba, K. Okitsu, H. Yamashita, T. Misawa, M. Tanaka, M. Kurihara, S. H. Gellman, *Org. Biomol. Chem.* **2015**, *13*, 5617–5620.
[28] S. J. Maynard, A. M. Almeida, Y. Yoshimi, S. H. Gellman, *J. Am. Chem. Soc.* **2014**, *136*, 16683–16688.
[29] M. Lee, N. Raman, S. H. Gellman, D. M. Lynn, S. P. Palecek, *ACS Chem. Biol.* **2014**, *9*, 1613–1621.
[30] Y. Shin, D. E. Mortenson, K. A. Satyshur, K. T. Forest, S. H. Gellman, *J. Am. Chem. Soc.* **2013**, *135*, 8149–8152.
[31] V. Semetey, D. Rognan, C. Hemmerlin, R. Graff, J–P. Briand, M. Marraud, G. Guichard, *Angew. Chem. Int. Ed.* **2002**, *41*, 1893–1895, *Angew. Chem. 114*, 1973–1975.
[32] A. Violette, M. C. Averland-Petit, V. Semetey, C. Hemmerlin, R. Casimir, R. Graff, M. Marraud, J–P. Briand, D. Rognan, G. Guichard, *J. Am. Chem. Soc.* **2005**, *127*, 2156–2164.
[33] L. Fischer, M. Decossas, J–P. Briand, C. Didierjean, G. Guichard, *Ang. Chem. Int. Ed.* **2009**, *48*, 1625–1628, *Angew. Chem. 121*, 1653–1656.
[34] A. Hennig, L. Fischer, G. Guichard, S. Matile, *J. Am. Chem. Soc.* **2009**, *131*, 16889–16895.
[35] P. Claudon, A. Violette, K. Lamour, M. Decossas, S. Fournel, B. Heurtault, J. Godet, Y. Mély, B. Jamart-Grégoire, M. C. Averlant-Petit, J. P. Briand, G. Duportail, H. Monteil, G. Guichard, *Angew. Chem. Int. Ed.* **2010**, *49*, 333–336, *Angew. Chem. 122*, 343–346.
[36] L. Fischer, P. Claudon, N. Pendem, E. Miclet, C. Didierjean, E. Ennifar, G. Guichard, *Angew. Chem. Int. Ed.* **2010**, *49*, 1067–1070, *Angew. Chem. 122*, 1085–1088.
[37] J. Fremaux, L. Fischer, T. Arbogast, B. Kauffmann, G. Guichard, *Angew. Chem. Int. Ed.* **2011**, *50*, 11382–11385, *Angew. Chem. 123*, 11548–11587.
[38] W. Collie, Gavin K. Pulka-Ziach, C. M. Lombardo, J. Fremaux, F. Rosu, M. Decossas, L. Mauran, O. Lambert, V. Gabelica, C. D. Mackereth, G. Guichard, *Nature Chem.* **2015**, *7*, 871–878.
[39] C. M. Lombardo, G. W. Collie, K. Pulka-Ziach, F. Rosu, V. Gabelica, C. D. Mackereth, G. Guichard, *J. Am. Chem. Soc.* **2016**, *138*, 10522–10530.
[40] G. W. Collie, R. Bailly, K. Pulka-Ziach, C. M. Lombardo, L. Mauran, N. Taib-Maamar, J. Dessolin, C. D. Mackereth, G. Guichard, *J. Am. Chem. Soc.* **2017**, *139*, 6128–6137.
[41] R. Wechsel, J. Raftery, D. Cavagnat, G. Guichard, J. Clayden, *Angew. Chem. In. Ed.* **2016**, *55*, 9657–9661, *Angew. Chem. 128*, 9809–9813.
[42] R. Wechsel, M. Zabka, J. W. Ward, J. Clayden, *J. Am. Chem. Soc.* **2018**, *140*, 3528–3531.
[43] R. Wechsel, J. Maury, J. Fremaux, S. P. France, G. Guichard, J. Clayden, *Chem. Comm.* **2014**, *50*, 15006–15009.
[44] N. Pendem, C. Douat, P. Claudon, M. Laguerre, S. Castano, B. Desbat, D. Cavagnat, E. Ennifar, B. Kauffmann, G. Guichard, *J. Am. Chem. Soc.* **2013**, *135*, 4884–4892.
[45] S. Durani, *Acc. Chem. Res.* **2008**, *41*, 1301–1308.
[46] V. Bobde, Y. U. Sasidhar, S. Durani, *Int. J. Pept. Protein Res.* **1994**, *43*, 209–218.
[47] A. Ehrlich, H.-U. Heyne, R. Winter, M. Beyermann, H. Haber, L. A. Carpino, M. Bienert, *J. Org. Chem.* **1996**, *61*, 8831–8838.
[48] S. Y. Hong, J. E. Oh, K. H. Lee, *Biochem. Pharmacol.* **1999**, *58*, 1775–1780.
[49] E. Krause, S. Rothemund, M. Beyermann, M. Bienert, *Anal. Chim. Acta* **1997**, *352*, 365–374.
[50] H. Weisshoff, C. Prasang, P. Henklein, C. Frommel, A. Zschunke, C. Mugge, *Eur. J. Biochem.* **1999**, *259*, 776–788.
[51] F. Formaggio, A. Bettio, V. Moretto, M. Crisma, C. Toniolo, Q. B. Broxterman, *J. Pept. Sci.* **2003**, *9*, 461–466.
[52] E. Krause, M. Beyermann, H. Fabian, M. Dathe, S. Rothemund, M. Bienert, *Int. J. Pept. Protein Res.* **1996**, *48*, 559–568.
[53] Y. Chen, C. T. Mant, R. S. Hodges, *J. Pept. Res.* **2002**, *59*, 18–33.
[54] Y. Inai, Y. Kurokawa, A. Ida, T. Hirabayashi, *Bull. Chem. Soc. Jpn.* **1999**, *72*, 55–61.
[55] M. M. Green, B. A. Garetz, B. Munoz, H. P. Chang, S. Hoke, R. G. Cooks, *J. Am. Chem. Soc.* **1995**, *117*, 4181–4182.
[56] M. M. Green, M. P. Reidy, R. J. Johnson, G. Darling, D. J. Oleary, G. Willson, *J. Am. Chem. Soc.* **1989**, *111*, 6452–6454.
[57] K. H. Mayo, E. Ilyina, H. Park, *Protein Sci.* **1996**, *5*, 1301–1315.
[58] D. Thirumalai, D. K. Klimov, R. I. Dima, *Curr. Opin. Struct. Biol.* **2003**, *13*, 146–159.
[59] J. S. Richardson, D. C. Richardson, *Proc. Natl. Acad. Sci. USA* **2002**, *99*, 2754–2759.
[60] Y. Takahashi, T. Yamashita, A. Ueno, H. Mihara, *Tetrahedron* **2000**, *56*, 7011–7018.
[61] B. K. Ho, A. Thomas, R. Brasseur, *Protein Sci.* **2003**, *12*, 2508–2522.
[62] C. Hemmerlin, M. Marraud, D. Rognan, R. Graff, V. Semetey, J. P. Briand, G. Guichard, *Helv. Chim. Acta* **2002**, *85*, 3692–3711.
[63] A.-Y. M. Woody, R. W. Woody, *Biopolymers* **2003**, *72*, 500–513.
[64] S. Bhattacharjee, G. Tóth, S. Lovas, J. D. Hirst, *J. Phys. Chem. B.* **2003**, *107*, 8682–8688.
[65] T. D. W. Claridge, *High-Resolution NMR Techniques in Organic Chemistry*; Elsevier Science: Amsterdam, 1999.
[66] F. Mohamadi, N. G. J. Richards, W. C. Guida, R. Liskamp, M. Lipton, C. Caufield, G. Chang, T. Hendrickson, W. C. Still, *J. Comput. Chem.* **1990**, *11*, 440–467.
[67] L. Baltzer, H. Nilsson, J. Nilsson, *Chem. Rev.* **2001**, *101*, 3153–3163.

Submitted: June 22, 2018
Accepted: October 10, 2018